Multi-body Heavy Meson Decay

David Asner

Carleton University, Department of Physics, 1125 Colonel By Drive, Ottawa, ON K1S 5B6, Canada

Abstract. Charm meson decay dynamics have been studied extensively over the last decade. Recently, B meson decay dynamics have also been analyzed. We describe the Dalitz-plot analysis technique which has been applied by many experiments to three-body D and B decays. We discuss results from the E791, FOCUS, CLEO, BABAR and BELLE experiments. These studies probe a variety of physics including charmless B-decay, doubly-Cabibbo suppressed decays, CP violation and T violation, the properties of established light mesons, charm spectroscopy and the properties of $\pi\pi$, $K\pi$ and KK S-wave states.

Keywords: charm,bottom,Dalitz
PACS: 13.25.Ft, 13.25.Hw, 11.80.Et

INTRODUCTION

Charm meson decay dynamics have been studied extensively over the last decade. Recent studies of multi-body decays of charm mesons probe a variety of physics including doubly-Cabibbo suppressed decays [1, 2], searches for CP violation [2, 3, 4, 5], T violation [6], D^0–$\overline{D}^0$ mixing [7], the properties of established light mesons [8, 9, 10, 11], the properties of $\pi\pi$ [1, 10, 12] $K\pi$ [13, 14], and KK [15] S-wave states, and the dynamics of four-body final states [16].

Recently, B meson decay dynamics have been studied. Multi-body decays of B mesons also probe a variety of physics including, charmless B-decays [17, 18, 19, 20, 21, 22, 23, 24], measurements of Cabibbo-Kobayashi-Maskawa (CKM) angle γ/ϕ_3 [25, 26, 27, 28], searches for direct CP violation [21, 22, 29], charm spectroscopy [30, 31], the properties of established light mesons [19, 22, 23], the properties of KK [19, 23] and $K\pi$ [19, 21, 22] S-wave, and the three-body production of baryons [20, 32]. Time-dependent Dalitz-plot (TD) analyses have been used to determine the CKM angle α/ϕ_2 [33]. A TD analysis of $B^0 \to D^{*\pm}K^0\pi^{\mp}$ [34] is sensitive γ/ϕ_3. Future studies could improve sensitivity to new physics in TD analyses of $b \to s$ penguin decays [23].

Weak nonleptonic decays of B and charm mesons are expected to proceed dominantly through resonant two-body decays in several theoretical models [35]; see Ref. [36] for a review of resonance phenomenology. These amplitudes are typically calculated with the Dalitz plot analysis technique [37], which uses the mininum number of independent observable quantities. For three-body final states when the parent particle is a scalar, the decay rate [38] is

$$\Gamma = \frac{1}{(2\pi)^3 32\sqrt{s^3}}\,|\mathscr{M}|^2\, dm_{12}^2 dm_{23}^2, \tag{1}$$

where m_{ij} is the invariant mass of $i-j$ and the coefficient of the amplitude includes all

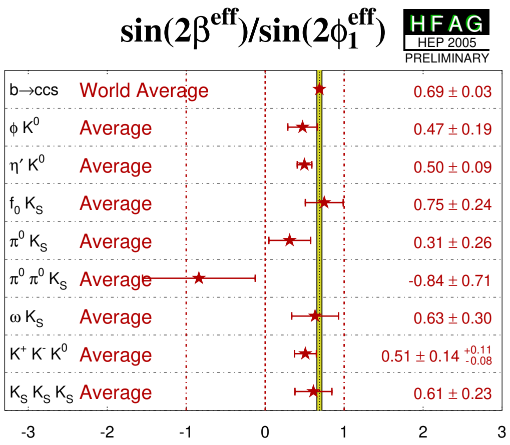

FIGURE 1. Comparison of results for $\sin 2\beta$ determined from $b \to c\bar{c}s$ and several $b \to s\bar{s}s$ processes.

kinematic factors. The scatter plot in m_{12}^2 versus m_{23}^2 is called a Dalitz plot. If $|\mathscr{M}|^2$ is constant, after efficiency correction and background subtraction, the allowed region of the plot will be populated uniformly with events. Any variation in $|\mathscr{M}|^2$ over the Dalitz plot is due to dynamical rather than kinematical effects. It is straightforward to extend the formalism beyond three-body final states. For N-body final states, phase space has dimension $3N-7$. Other cases of interest include one vector particle or a baryon/anti-baryon pair in the final state. For the former case phase space has dimension $3N-5$ and for the latter $3N-4$.

CHARMLESS *B*-DECAY

Several charmless three-body final states have been analyzed by Babar and Belle: $B^+ \to K^+\pi^-\pi^+$ [18, 19, 22], $B^+ \to K^+K^-K^+$ [19], $B^+ \to \pi^+\pi^-\pi^+$ [24], $B^0 \to K^+\pi^-\pi^0$ [21], $B^0 \to K_S^0\pi^+\pi^-$ [17], $B^0 \to K_S^0K^+K^-$ [23] and $B^0 \to \pi^+\pi^-\pi^0$ [33]. These final states are also accessible in D decay and the resonant substructure is modelled following Ref. [3]. The available phase space is much large in B decay and more sophisticated descriptions of the non-resonant contribution are under development. The study of the $\pi\pi$, $K\pi$, KK S-wave at CLEO-c from hadronic charmonium decay, which spans most of the phase space of interest, may provide important input. As in D decay, no strong evidence for direct CP violation has been observed.

Charmless three-body decays of the B meson are a rich laboratory providing information on the weak sector and the dynamics of strong interactions. Decays to the final state $K_S^0K^+K^-$ are dominated by the $b \to s\bar{s}s$ amplitudes and are of particular interest due their sensitivity to physics beyond the Standard Model. This Dalitz-plot is dominated by a non-resonant KK S-wave component and in the low mass KK region a significant P-wave contribution from ϕK_S^0.

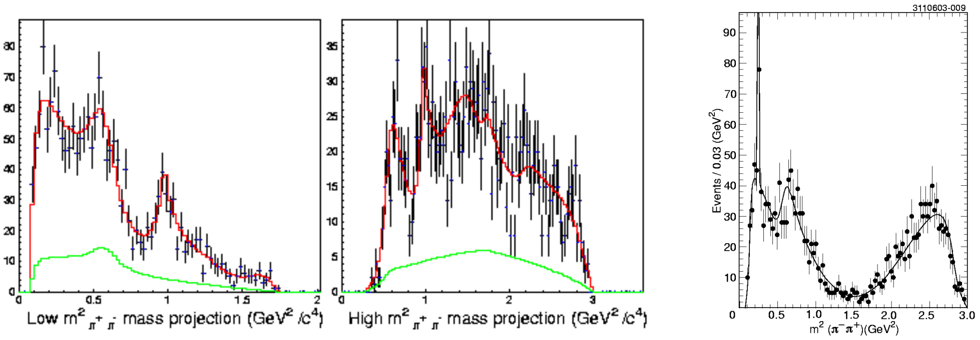

FIGURE 2. $\pi^+\pi^-$ projection of Left: $D^+ \to \pi^+\pi^-\pi^+$ (low mass) and Center: $D^+ \to \pi^+\pi^-\pi^+$ (high mass) from FOCUS [10]. Right: $D^0 \to \pi^+\pi^-\pi^0$ from CLEO [5]. The D^0 final state is consistent with the absence of $\pi\pi$ S-wave while this amplitude dominates the D^+ final state. Data (points) and total fit (curve) are shown. The background contribution for $D^+ \to \pi^+\pi^-\pi^+$ is also shown

The CKM parameter $\sin 2\beta$ can be determined from the time-dependent CP asymmetry in several $b \to s$ penguin processes. These are compared, in Fig. 1, to the precision measurement from $b \to c\bar{c}s$ which is dominated by $B^0 \to \psi K_S$.

TIME-DEPENDENT DALITZ-PLOT ANALYSIS

$B^0 \to \pi^+\pi^-\pi^0$ and $\sin 2\alpha$: The $B^0 \to \pi^+\pi^-\pi^0$ Dalitz plot is dominated by ρ intermediate resoanances. Although $\rho\pi$ is not a CP eigenstate, the time-dependent analysis of this Dalitz plot allows simultaneous determination of the strong transition amplitudes and phases and the CKM angle α. Using 213 million $\Upsilon(4S) \to B\bar{B}$ decays BABAR finds $\alpha = (113^{+27}_{-17} \pm 6)^o$ [33] and 2.9σ evidence for direct CP violation.

$D^0 \to K^0_S\pi^+\pi^-$ and Search for $D^0 - \overline{D}^0$ Mixing: The resonant substructure of $D^0 \to K^0_S\pi^+\pi^-$ can be described by a combination of ten quasi two-body intermediate states which include both CP-even and CP-odd eigenstates and one doubly Cabibbo suppressed channel. The time-dependent analysis of this Dalitz plot allows simultaneous determination of the strong transition amplitudes and phases and the mixing parameters x and y without phase or sign ambiguity. Using 9 fb^{-1}, CLEO II.V constrains $(-4.5 < x < 9.3)\%$ and $(-6.4 < y < 3.6)\%$ [7].

Search for New Physics in $b \to s$ Penguin Processes: A time-dependent Dalitz-plot analysis of the $b \to s$ penguin processes listed in Fig. 1 has not been done. Most $b \to s$ penguin final states, such as $K^+K^-K^0_S$, are not pure CP eigenstates. A time-dependent analysis of this Dalitz plot would allow the simultaneous determination of the strong transition amplitudes and phases and the CKM angle β while reducing the systematic uncertainties associated with selecting ϕK^0_S from $K^+K^-K^0_S$. A precision measurement of $\sin 2\beta$ in $b \to s$ penguin processes is required to establish a discrepancy between $\sin 2\beta$ determined with $b \to c\bar{c}s$ and $b \to s\bar{s}s$ which might be attributed to new physics.

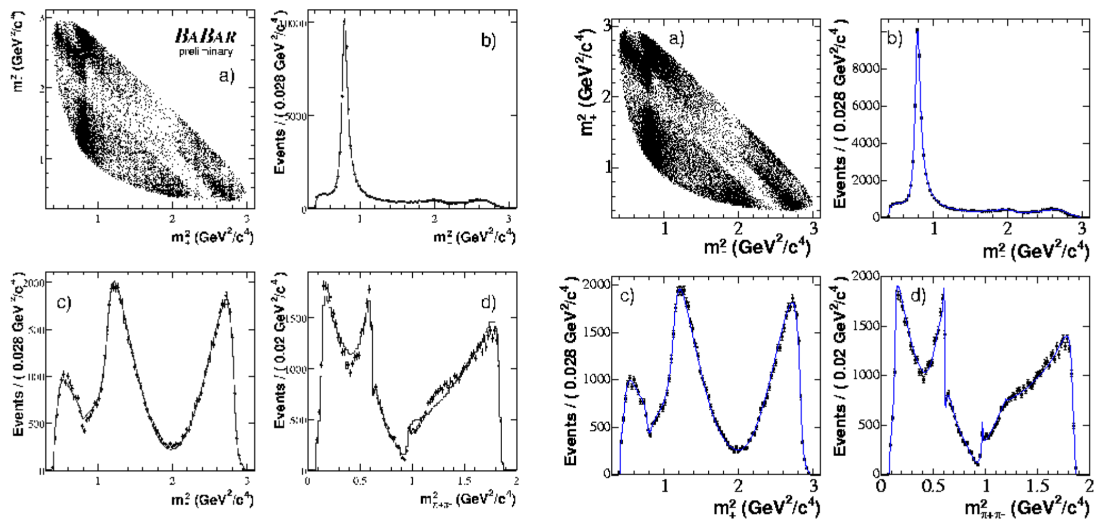

FIGURE 3. Dalitz plot of $D^0 \to K^0_S\pi^+\pi^-$ [28]. Left: Breit-Wigner model [1] does describe the $\pi\pi$ projection of the BABAR data. Right: K-matrix parameterization of $\pi\pi$ S-wave yields much improved fit.

DETERMINING γ/ϕ_3 FROM $B^- \to DK^-, D \to K^0_S\pi^+\pi^-$

Various approaches have been proposed to measure γ/ϕ_3 in $B^\mp \to DK^\mp$ decays [39, 40, 41, 42, 43, 44]. The Dalitz-plot analysis of three-body D^0 decay from $B^\mp \to DK^\mp$ provides the best measurement of γ/ϕ_3. This approach suffers from the Dalitz-plot model uncertainty introduced by the unknown complex phase of D^0 decay. Recently Babar [45] and Belle [46] have reported $\gamma = (70 \pm 31^{+12+14}_{-10-11})^\circ$ and $\phi_3 = (77^{+17}_{-19} \pm 13 \pm 11)^\circ$, respectively, where the third error is the systematic error due to modeling of the Dalitz plot. With larger data samples soon to be available, this uncertainty is expected to be dominant in the γ/ϕ_3 measurement.

The senstivity to γ/ϕ_3 is due to the interference of two amplitudes producing opposite flavors of D mesons. In the case of B^+ decay, the state $D_+ = D^0 + re^{i\theta_+}\overline{D}^0$ where r is the ratio of doubly-Cabbib suppressed to Cabibbo favored amplitude and the relative phase between D^0 and $\overline{D}^0$ is $\theta_+ = \gamma/\phi_3 + \delta$. Analogously for B^-, $D_- = \overline{D}^0 + re^{i\theta_-}D^0$ with $\theta_- = -\gamma/\phi_3 + \delta$

The CLEO-c physics program includes a variety of measurements that will improve the determination of γ/ϕ_3 from the B-factory experiments. The total number of charm mesons accumulated at CLEO-c will be much smaller than the samples already accumulated by the B-factories. However, the quantum correlation of $D\bar{D}$ system from $\psi(3770)$ and $E \sim 4160$ MeV provides a unique laboratory in which to study charm in general and models of multibody charm decay in particular. It has been shown [47] that the Dalitz-plot model uncertainty can be reduced utilizing a sample of D^0 in a CP eigenstate. This sample is being accumulated at CLEO-c from the processes $e^+e^- \to \psi(3770) \to D\bar{D} \to (CP\pm)(K^0_S\pi^+\pi^-)$. It is estimated that a sample of 1 fb^{-1} of integrated luminosity at the $\psi(3770)$ would allow the measurement of γ/ϕ_3 to a precision of a few degrees.

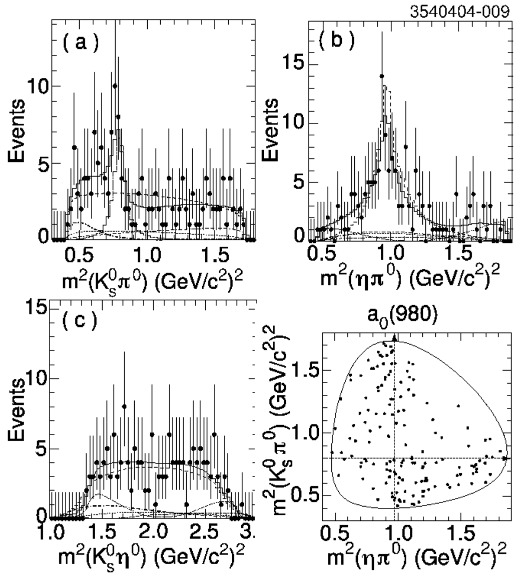

FIGURE 4. The three projections and the $D^0 \to K_S^0\eta\pi^0$ Dalitz plot. The fit to CLEO data [11] has contributions from $a_0(980)K_S^0$, $K^*(892)\eta$, $K_0^*(1430)\eta$, and $a_2(1320)K_S^0$.

K-MATRIX FORMALISM

Usually the resonances in Dalitz-plot analyses are modeled with a Breit-Wigner and the nonresonant contribution $D \to abc$ is parameterized as an S-wave with no variation in magnitude or phase across the Dalitz plot. Some more recent analyses have used the K-matrix formalism [48] with the P-vector approximation [49] to describe the $\pi\pi$ S-wave.

The decay $D^+ \to \pi^+\pi^+\pi^-$, dominated by $\pi\pi$ S-wave, has been studied by the E687 [8], E791 [12] and FOCUS [10] experiments. FOCUS analyzed its data sample using both the Breit-Wigner formalism and the K-matrix formalism, following the 5 pole, 5 resonance model of Anisovich and Sarantsev [51]. The Breit-Wigner analysis included $\rho(770), f_0(980), f_2(1270), f_0(1500), \sigma(500)$, and a nonresonant contribution. Applying the K-matrix formalism to the S wave and parameterizing the $\rho(770)$ and $f_2(1270)$ with the Breit-Wigner functions also described the FOCUS data well. The K-matrix fit to the FOCUS data is shown in Fig. 2.

The decay $D^0 \to \pi^+\pi^-\pi^0$, dominated by $\pi\pi$ P-wave, has been studied by the CLEO experiment. Only the three $\rho(770)\pi$ resonant contributions are observed. No evidence is found for $\pi\pi$ S-wave with either the Breit-Wigner or a K-matrix parameterization, following the 4 pole, 2 resonance model of Au, Morgan, and Pennington [50]. The K-matrix fit to the CLEO data is shown in Fig. 2.

The decay $D^0 \to K_S^0\pi^+\pi^-$, important for the determination of γ/ϕ_3, has been studied by several experiments. The CLEO model [1] (includes $\rho(770)$, ω, $f_0(980)$, $f_2(1270)$, $f_0(1370)$, $K^*(892)^-$, $K_0(1430)^-$, $K_2(1430)^-$, $K^*(1680)^-$ and the doubly-Cabibbo suppressed amplitude $K^(892)^+$ as well as a small non-resonant component) does not provide a good description of the BABAR data. An improved description is obtain in two ways. First, by adding additional Breit-Wigner resonances including two arbitrary $\pi\pi$

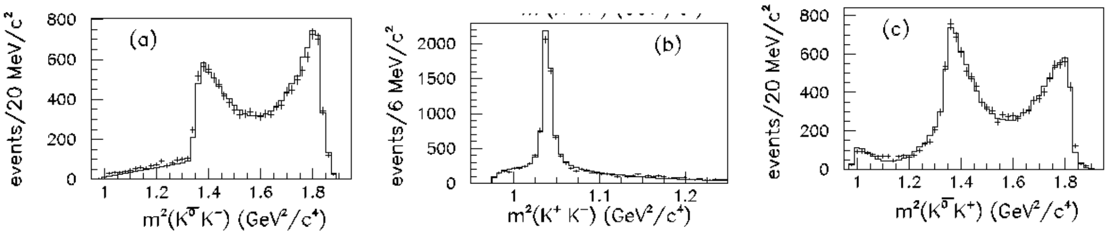

FIGURE 5. Projections of the BABAR data and fit to the $D^0 \to K^0_S K^+ K^-$ Dalitz plot [15].

resonances, σ_1 and σ_2. Second, following the methodology of FOCUS, BABAR has applied a K-matrix model to describe the $\pi\pi$ S-wave [28]. Both the Breit-Wigner fit and the K-matrix fit are shown in Fig. 3.

STUDYING LOW MASS $\pi\pi$, $K\pi$, KK S-WAVE

The meson content of the 0^{++} of nonet and the quark content of the $f_0(980)$, $a_0(980)$, $f_0(1370)$, $f_0(1500)$, and $f_0(1710)$ mesons are current puzzles in light meson spectroscopy. Measuring branching fractions and couplings to different final states and the comparison of scalar meson production rates among D^0, D^+ and D_s^+ mesons may help resolve these issues.

An interesting example of studies of 0^{++} mesons in D decays follows. A large contribution of $f_0(980)$ to $D^0 \to K^0_S K^+ K^-$ was reported by ARGUS [52] and BABAR [53]. This is inconsistent with the smaller contribution of $f_0(980)$ observed in $D^0 \to K^0_S \pi^+ \pi^-$ [1]. One possible explanation is that the $D^0 \to K^0_S K^+ K^-$ has a large contribution from $a_0(980) \to K^+ K^-$. The CLEO collaboration was motivated to study $D^0 \to K^0_S \eta \pi^0$ where the dominant contribution is from $K^0_S a_0(980), a_0(980) \to \eta\pi$ and no contribution from $f_0(980)$. The CLEO data and projection of fit results are shown in Fig. 5. A more recent analysis from BABAR includes a large contribution from $a_0(9800 \to KK$ and little $f_0(980)$ [15].

Indication of a broad $K\pi$ scalar intermediate resonance has been reported by E791 in

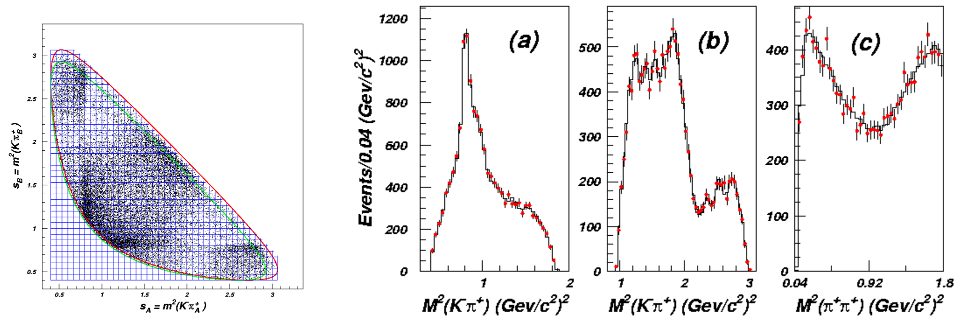

FIGURE 6. Left: Dalitz plot of $D^+ \to K^- \pi^+ \pi^+$ in E791 data [14]. (a) Low mass $K\pi$ (b) high mass $K\pi$ (c) $\pi\pi$ projections.

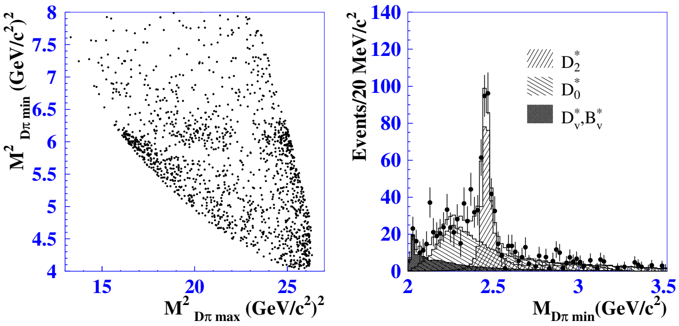

FIGURE 7. Left: Dalitz plot $B^0 \to D^0\pi^+\pi^-$ from Belle [30], . Right: Low mass $D^0\pi$ projection of data and components fit.

the decay $D^+ \to K^-\pi^+\pi^+$ [13]. Fitting the Dalitz plot with $\overline{K}^*(892)^0\pi^+$, $\overline{K}_0^*(1430)^0\pi^+$, $\overline{K}_2^*(1430)^0\pi^+$, and $\overline{K}^*(1680)^0\pi^+$, plus a constant nonresonant component, E791 finds results consistent with earlier results [54, 55] with a nonresonant fit fraction of over 90%. Having reconstructed more events than the other experiments, E791 was led to include an extra low-mass S-wave $\overline{K}\pi$ resonance to account for the poor fit already seen by earlier experiments: A $\kappa(800)$ with $m = 797 \pm 19 \pm 43$ MeV/c^2 and $\Gamma = 410 \pm 43 \pm 87$ MeV/c^2 much improved the fits. The $\kappa(800)$ is now the dominant resonance and the nonresonant fit fraction is reduced from $90.9 \pm 2.6\%$ to $13.0 \pm 5.8 \pm 4.4\%$.

E791 also modeled the $K\pi$ S-wave phase variation as a function of $K\pi$ mass with the $K_0^*(1430)$ resonance only and a nonresonant component following the parameterization of LASS [56]. It was necessary to relax the unitarity constraint to describe the E791 data [13]. The $K\pi$ S-wave phase behavior in this model is consistent with the model that includes the κ resonance.

Finally, E791 performed a model independent partial wave analysis (MIPWA) of the S-save component of the $K\pi$ system. The amplitude and phase for the $K\pi$ S-wave are obtained from $K\pi$ threshold up to 1.72 GeV/c^2. The S-wave amplitudes require no assumptions about its dependence on invariant mass, but do rely on the relatively well understood P-wave and D-wave. The P-wave is described by the $K^*(892)$ and $K^*(1680)$

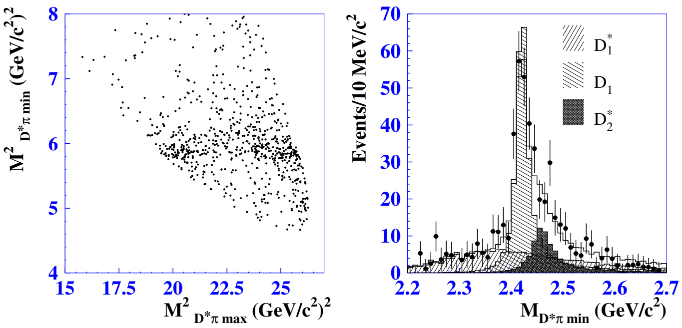

FIGURE 8. Left: Dalitz plot $B^0 \to D^{*+}\pi^+\pi^-$ from Belle [31], . Right: Low mass $D^{*+}\pi$ projection of data and components fit.

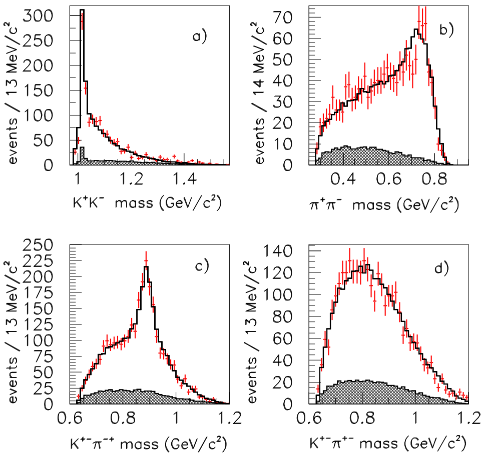

FIGURE 9. Projections of $D^0 \to K^+K^-\pi^+\pi^-$ from FOCUS [16]. a) KK b) $\pi\pi$ c) $K^{\pm}\pi^{m}p$ d) $K^{\pm}\pi^{-}\pm$. Data (points), total fit (histogram) and background (shaded) are shown.

and the D-wave is described by the $K_2(1430)$ parameterized as Breit-Wigner resonances. The results of the MIPWA are shown in Fig. 6 and provide a similar description of the data as Ref. [13] which parametrized the S-wave with a κ and $K_0(1430)$ Breit-Wigner resonances and a constant complex non-resonant term.

BEYOND $P \to 3P$ DECAYS

Charm Spectroscopy: The decay $B \to D\pi\pi$ where the D is fully recontructed can be analyzed with the usual Dalitz-plot analysis technique for $P \to 3P$ decays. The Dalitz-plot for this process from Belle [30], is shown in Fig 7. The spin-structure of the narrow D_2^* is evident. In addition to the relative amplitude and phase, the mass and width of the narrow D_2^* and broad D_0^* are determined in the Dalitz-plot fit. The data and projection of the components of the Dalitz-plot fit on to the $m_{D\pi}$ minimum mass is shown in Fig. 7.

The decay $B \to D^*\pi\pi$ where the D^* is fully reconstructed has two additional degrees of freedom, assuming the width of the D^{*+} to be negligible [57]. In addition to the Dalitz-plot variables $(m_{D^{*+}\pi^+}, m_{D^{*+}\pi^-})$ one can choose the variables to be the angle between the pions in the D^{*+} rest frame and the azimuthal angle of the pion from the D^{*+} relative to the $D^{*+}\pi\pi$ decay plane. The Dalitz-plot from Belle [31], is shown in Fig. 8. In addition to the relative amplitudes and phases the mass and width of D_1^0 and $D_1'^0$ are determined. The parameters for D_2^* are fixed from the $B \to D\pi\pi$ analysis. The data and projection of the components of the fit on to the $m_{D^*\pi}$ minimum mass is shown in Fig. 8.

$D \to KK\pi\pi$: The FOCUS experiment has extended the Dalitz-plot formalism to analyze $D^0 \to K^+K^-\pi^+\pi^-$ with four pseudoscalars in the final state. Final states produced through spectator amplitudes in which the W is coupled to a vector (V) or axial-vector

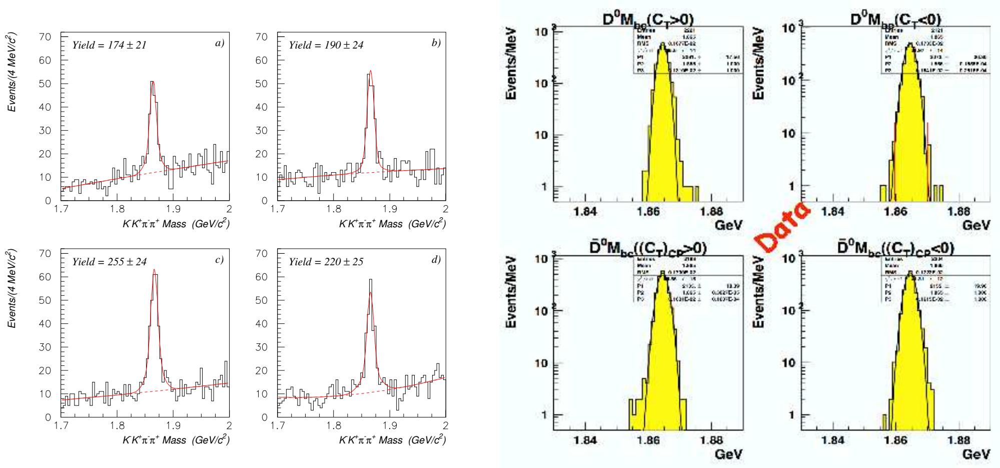

FIGURE 10. Top Row: Invariant mass for $D^0 \to K^+K^-\pi^+\pi^-$ candidates. Bottom Row: Invariant mass for $\overline{D}^0 \to K^+K^-\pi^+\pi^-$ candidates. No indication of T violation is observed in the FOCUS data (left) [6] or CLEO-c data (right).

(A) meson are expected to dominate over those where the W is coupled to a pseudoscaler (P) meson. The dominant contribution to the rate (55%) is from the $D^0 \to AP$ modes, $K_1(1270)^-K^+$ and $K_1(1400)^-K^+$, a large contribution ($\sim 30\%$) from $D^0 \to VV$ modes, mostly $\phi\rho$. The remaining contributions are from $D^0 \to VPP$ and $D^0 \to SPP$, primarily from $K^*(892)^0K^+\pi^-$ and $f_0(980)\pi^+\pi^-$. The projections of the data and fit are shown in Fig. 9.

Search for T-Violation: The FOCUS experiment has searched for T violation four-body charm meson decays using the channels $D^0 \to K^+K^-\pi^+\pi^-$, $D^+ \to K^0_S K^+\pi^-\pi^+$, and $D_s^+ \to K^0_S K^+\pi^-\pi^+$ [6]. The T violation asymmetry is defined as $A_{Tviol} \equiv (A_T - \bar{A}_T)$ where A_T is defined as $A_T \equiv \frac{\Gamma(\vec{v}_1 \dot{(} \vec{v}_2 \times \vec{v}_3) > 0) - \Gamma(\vec{v}_1 \dot{(} \vec{v}_2 \times \vec{v}_3) < 0)}{\Gamma(\vec{v}_1 \dot{(} \vec{v}_2 \times \vec{v}_3) > 0) + \Gamma(\vec{v}_1 \dot{(} \vec{v}_2 \times \vec{v}_3) < 0)}$ where each v_i is a momentum which are odd under time reversal. They report $A_{Tviol}(D^0) = 0.010 \pm 0.057 \pm 0.037$, $A_{Tviol}(D^0) = 0.023 \pm 0.062 \pm 0.022$, and $A_{Tviol}(D_s^+) = -0.036 \pm 0.067 \pm 0.023$. The FOCUS and CLEO-c $D^0 \to K^+K^-\pi^+\pi^-$ invariant mass distributions are compared in Fig. 10. In 281 pb^{-1} CLEO-c sample is nearly background freewith $\sim$10 times the signal yield of FOCUS. CLEO-c has not reported results for A_{Tviol}.

REFERENCES

1. H. Muramatsu *et al.* [CLEO Collaboration], Phys. Rev. Lett. **89**, 251802 (2002) [Erratum-ibid. **90**, 059901 (2003)].
2. G. Brandenburg *et al.* [CLEO Collaboration], Phys. Rev. Lett. **87**, 071802 (2001).
3. S. Kopp *et al.* [CLEO Collaboration], Phys. Rev. D **63**, 092001 (2001).
4. D. M. Asner *et al.* [CLEO Collaboration], Phys. Rev. D **70**, 091101 (2004).
5. D. Cronin-Hennessy *et al.* [CLEO Collaboration], Phys. Rev. D **72**, 031102 (2005).
6. J. M. Link *et al.* [FOCUS Collaboration], Phys. Lett. B **622**, 239 (2005).
7. D. M. Asner [CLEO Collaboration], Phys. Rev. D **72**, 012001 (2005).

8. P. L. Frabetti *et al.* [E687 Collaboration], Phys. Lett. B **407**, 79 (1997).
9. E. M. Aitala *et al.* [E791 Collaboration], Phys. Rev. Lett. **86**, 765 (2001).
10. J. M. Link *et al.* [FOCUS Collaboration], Phys. Lett. B **585**, 200 (2004).
11. P. Rubin *et al.* [CLEO Collaboration], Phys. Rev. Lett. **93**, 111801 (2004).
12. E. M. Aitala *et al.* [E791 Collaboration], Phys. Rev. Lett. **86**, 770 (2001).
13. E. M. Aitala *et al.* [E791 Collaboration], Phys. Rev. Lett. **89**, 121801 (2002).
14. E. M. Aitala *et al.* [E791 Collaboration], arXiv:hep-ex/0507099.
15. B. Aubert *et al.* [BABAR Collaboration], Phys. Rev. D **72**, 052008 (2005).
16. J. M. Link *et al.* [FOCUS Collaboration], Phys. Lett. B **610**, 225 (2005).
17. K. Abe *et al.* [Belle Collaboration], arXiv:hep-ex/0509047.
18. K. Abe [Belle Collaboration], arXiv:hep-ex/0509001.
19. A. Garmash *et al.* [BELLE Collaboration], Phys. Rev. D **71**, 092003 (2005).
20. K. Abe *et al.* [BELLE Collaboration], arXiv:hep-ex/0409010.
21. B. Aubert *et al.* [BABAR Collaboration], arXiv:hep-ex/0408073.
22. B. Aubert *et al.* [BABAR Collaboration], arXiv:hep-ex/0507004.
23. B. Aubert *et al.* [BABAR Collaboration], arXiv:hep-ex/0507094.
24. B. Aubert *et al.* [BABAR Collaboration], arXiv:hep-ex/0408032.
25. A. Poluektov *et al.* [Belle Collaboration], Phys. Rev. D **70**, 072003 (2004).
26. K. Abe *et al.* [Belle Collaboration], arXiv:hep-ex/0411049.
27. K. Abe *et al.* [Belle Collaboration], arXiv:hep-ex/0504013.
28. B. Aubert *et al.* [BABAR Collaboration], arXiv:hep-ex/0507101.
29. A. Garmash, arXiv:hep-ex/0505048.
30. K. Abe *et al.* [Belle Collaboration], Phys. Rev. D **69**, 112002 (2004).
31. K. Abe *et al.* [Belle Collaboration], arXiv:hep-ex/0412072.
32. K. Abe *et al.* [BELLE Collaboration], arXiv:hep-ex/0409005.
33. B. Aubert *et al.* [BABAR Collaboration], arXiv:hep-ex/0408099.
34. B. Aubert *et al.* [BABAR Collaboration], arXiv:hep-ex/0412040.
35. M Bauer, B. Stech and M. Wirbel, Z. Phys. C **34**, 103 (1987); P. Bedaque, A. Das and V.S. Mathur, Phys. Rev. D **49**, 269 (1994); L.-L. Chau and H.-Y. Cheng, Phys. Rev. D **36**, 137 (1987); K. Terasaki, Int. J. Mod. Phys. A **10**, 3207 (1995); F. Buccella, M. Lusignoli and A. Pugliese, Phys. Lett. B **379**, 249 (1996).
36. J. D. Jackson, Nuovo Cim. **34**, 1644 (1964).
37. R. H. Dalitz, *Phil. Mag.* **44**, 1068 (1953).
38. See the review on Kinematics revised by J. D. Jackson on Page 675-679 of the Review of Particle Physics, Phys.Lett.B592: 1,2004.
39. M. Gronau and D. London., Phys. Lett. B **253**, 483 (1991).
40. M. Gronau and D. Wyler, Phys. Lett. B **265**, 172 (1991).
41. I. Dunietz, Phys. Lett. B **270**, 75 (1991).
42. D. Atwood, G. Eilam, M. Gronau and A. Soni, Phys. Lett. B **341**, 372 (1995).
43. D. Atwood, I. Dunietz and A. Soni, Phys. Rev. Lett. **78**, 3257 (1997).
44. D. Atwood, I. Dunietz and A. Soni, Phys. Rev. D **63**, 036005 (2001).
45. B. Aubert *et al.* [BABAR Collaboration], f arXiv:hep-ex/0504039.
46. K. Abe *et al.* [Belle Collaboration], arXiv:hep-ex/0504013.
47. A. Giri, Y. Grossman, A. Soffer and J. Zupan, Phys. Rev. D **68**, 054018 (2003).
48. S.U. Chung *et al.*, Ann. Physik. **4**, 404 (1995).
49. I. J. R. Aitchison, Nucl. Phys. **A 189**, 417 (1972).
50. K. L. Au, D. Morgan and M. R. Pennington, Phys. Rev. D **35**, 1633 (1987).
51. V. V. Anisovich and A. V. Sarantsev, Eur. Phys. J. A **16**, 229 (2003).
52. H. Albrecht *et al.* [ARGUS Collaboration], Z. Phys. C **33**, 359 (1987).
53. B. Aubert *et al.* [BABAR Collaboration], arXiv:hep-ex/0207089.
54. J.C. Anjos *et al.* [E691 Collaboration], Phys. Rev. D**48** 56 (1993).
55. P.L. Frabetti *et al.* [E687 Collaboration], Phys. Lett. B**331**, 217 (1994).
56. D. Aston *et al.* [LASS Collaboration], Nucl. Phys. B **296**, 493 (1988).
57. A. Anastassov *et al.* [CLEO Collaboration], Phys. Rev. D **65**, 032003 (2002).